Supporting Information

Hierarchical Porous Organometallic Polymers Enable Industrial-level Acidic CO_2 Electroreduction

Weitao Ji[†1,2], Boxuan Liu[†2], Jiaji Zhang[1,2], Jie Zhu[1,2], Wenhua Zhou[1,2], Teng Guo[1,2], Lei Guo[1,2], Xilin Jiang[2], Ming Ya[1,2], Zhenyu Zhang[1,2], Huiping Ji[1,2], Jianghao Wang[1,2], Yajing Shen*[1,2], Bolong Li[1,2], Jie Fu*[1,2]*

[1]Key Laboratory of Biomass Chemical Engineering of Ministry of Education, College of Chemical and Biological Engineering, Zhejiang University, Hangzhou 310058, China

[2] Zhejiang Key Laboratory of Green Biomanufacturing of Functional Sugar Alcohols, Institute of Zhejiang University-Quzhou, 99 Zheda Road, Quzhou 324000, China

[*]**Corresponding author**

Jianghao Wang*: wjh7744@zju.edu.cn

Yajing Shen*: yajshen@zju.edu.cn

Jie Fu*: jiefu@zju.edu.cn

† These authors contributed equally to this work.

Experimental sections

Chemical and materials.

Potassium bicarbonate ($KHCO_3$, AR) and Formaldehyde dimethyl acetal (FDA, 98%) were purchased from the Shanghai Aladdin Biochemical Technology Co., Ltd. Cobalt Phthalocyanine (CoPc,>90%) were supplied by Shanghai Macklin Biochemical Co., Ltd. 1,2-Dichloroethane (DCE, AR), Anhydrous Ferric Chloride ($FeCl_3$, CP), Benzene (AR) Methanol (AR), Ethanol (AR), Isopropanol (AR), Potassium Sulfate (K_2SO_4, AR), Sulfuric Acid (H_2SO_4, AR) were purchased from Sinopharm Chemical Reagent Co., Ltd. The conductive carbon black VXC-72R was obtained from Tianjin EVS Chemical Technology Co., Ltd. Dupont Nafion solution (D520), Cation exchange membrane (CEM) Nafion 117 and titanium electrode coated with iridium oxide were purchased from Suzhou Sineruo Technology Co., Ltd. Saturated calomel electrode and Ag/AgCl electrode were purchased from Gaoss Union Technology Co., Ltd. 28 BC carbon paper used for preparing the working electrode was purchased from SGL CARBON SE. All chemicals were used without any purification. All aqueous solution was prepared using ultrapure water (>18 MΩ cm).

Synthesis of CoPc POPs. The synthesis method of CoPc POPs is similar to those reported in previous works. For CoPc-POP-c, 0.1 mmol of cobalt phthalocyanine and 1 mmol of benzene were added to a Schlenk tube containing 1 mL of anhydrous 1,2-dichloroethane (DCE). After sonicating for 10 minutes, 2 mmol of anhydrous ferric chloride and 2 mmol of formaldehyde dimethyl acetal (FDA) were introduced under a nitrogen atmosphere. The

mixture was then heated to 80°C and stirred for 24 hours under nitrogen protection. After cooling to room temperature, the resulting fluffy solid was collected and washed multiple times with methanol, deionized water, dichloromethane, and acetone. The product was further purified by Soxhlet extraction with methanol at 95°C for 48 hours. Finally, the solid was dried under vacuum at 60°C for 24 hours to give a dark blue powder. The preparation of CoPc-POP-a-b and d-g is similar to that of CoPc-POP-c, with the only differences being the varying amounts of benzene, anhydrous $FeCl_3$, and FDA added. The specific ratios can be found in Table S1.

Characterizations.

X-ray powder diffraction (XRD) analysis was performed using a Rigaku Ultimate IV instrument to investigate phase transitions during the synthesis process. The measurements utilized Cu Kα radiation (λ = 1.5418 Å) at operating conditions of 40 kV and 40 mA. Additionally, XRD measurements for comparing structural changes before and after the CO_2RR were conducted directly on the carbon paper. The morphology and elemental distribution were characterized using field emission scanning electron microscopy (SEM, Hitachi Regulus 8230) and transmission electron microscopy (TEM, Thermo Fisher Scientific Talos F200X). The specific surface area and pore size distribution of the catalyst were determined using a Micromeritics 3Flex instrument based on the Brunauer-Emmett-Teller (BET) method. The cobalt content in the catalyst and post-electrolysis solution was quantified using an inductively coupled plasma optical emission spectrometer (ICP-OES, Agilent 720ES).

Fourier-transform infrared (FT-IR) spectra were recorded on a Thermo Nicolet IS50 spectrometer with KBr pellets. X-ray photoelectron spectroscopy (XPS) measurements were conducted using a Shimadzu Kratos AXIS Supra+. X-ray absorption fine structure (XAFS) spectroscopy was carried out using the RapidXAFS 2M (Anhui Absorption Spectroscopy Analysis Instrument Co., Ltd.) by transmission mode at 20 kV and 20 mA, and the Si (511) spherically bent crystal analyzer with a radius of curvature of 500 mm was used for Cr.

Preparation of the working electrode

The catalyst for testing consisted of conductive carbon black and CoPc POPs. To prepare electrodes with different carbon contents, carbon black and CoPc POPs were mixed at mass ratios of 1:9, 3:7, 5:5, 7:3, and 9:1, with the total catalyst mass fixed at 10 mg. The mixture was then dispersed in 1 mL of a solution containing 750 μL isopropanol, 200 μL deionized water, and 50 μL Nafion, resulting in a catalyst ink concentration of approximately 10 mg mL^{-1}. The ink was sonicated for 30 minutes to ensure uniform dispersion. The catalyst ink was evenly sprayed in four passes onto a 2.25 cm × 2.25 cm (about 5 cm^2) piece of 28BC carbon paper using a spray gun. During spraying, the remaining ink was continuously sonicated to prevent carbon black sedimentation. After spraying, the electrode was air-dried overnight. The final catalyst loading was approximately 1.5 mg cm^{-2}.

Electrochemical measurements.

In this work, CHI 760E and CHI 1140D electrochemical workstations (CH Instruments, Inc., Shanghai) were used for electrochemical measurements. The electrochemical experiments were conducted in a custom-made flow electrolysis cell, with all compartments having circular cross-sections and a cross-sectional area of 2 cm^2. The counter electrode consisted of titanium felt coated with iridium dioxide (IrO_2). The Nafion 117 were used as the ion exchange membrane in neutral and acidic solutions. A saturated calomel electrode (SCE) was chosen as the reference electrode. Under acidic conditions, 0.25 M K_2SO_4 electrolyte adjusted to pH=1 with sulfuric acid, served as the electrolyte. During the test, the anolyte and catholyte were circulated between their respective chambers and electrolyte reservoirs using peristaltic pumps at a flow rate of 5 mL min^{-1}. For each test, 300 mL of fresh electrolyte was added to both the anode and cathode reservoirs. All potentials of this work were calibrated with respect to RHE without iR correction:

$$E\ (\text{vs. RHE}) = E\ (\text{vs. } Hg/Hg_2Cl_2) + 0.241\ V + 0.0591\ V \times pH$$

Linear sweep voltammetry (LSV) measurements under different atmospheric conditions were conducted in a flow cell using a 0.25 M K_2SO_4 electrolyte acidified with sulfuric acid, at a scan rate of 10 mV/s. The electrochemically active surface area (ECSA) of the electrode was determined by measuring the double-layer capacitance (C_{dl}). The C_{dl} was estimated by plotting the $\Delta j/2$ at open circuit potential against the scan rates, in which the Δj are the differential between the anodic and cathodic current densities. The scan rate was incrementally increased from 20 to 100 mV/s in uniform steps. The electrochemical impedance spectroscopy (EIS) measurement was carried out with an amplitude of 5 mV from 1 to 10^5 Hz.

Product analysis.

During the electrolysis process, CO_2 gas was directly introduced into the cathode compartment at a flow rate of 30 sccm, regulated by a precision mass flow controller. The outlet gas flow rate was corrected using a soap film flowmeter and subsequently analyzed and quantified using a gas chromatograph (Agilent 8860 GC system). A thermal conductivity detector (TCD) was employed for H_2 detection, while a flame ionization detector (FID) was utilized for CO detection.

The Faraday efficiency of gas-phase products is calculated according to the following formula:

$$FE = \frac{j_i}{j_{total}} = \frac{n_i NF}{j_{total}}$$

F represents the Faraday constant, with a value of 96485 C mol^{-1}; j_{total} represents the total current; j_i denotes the partial current for CO or H_2 production; n_i is the production rate of CO and H_2; N refers to the number of electrons involved in the formation of CO and H_2.

The n_i can be calculated as:

$$n_i = \frac{PV_i}{RT}$$

V_i represents the flow rate of CO and H_2 in the outlet gas, and it can be calculated as follows:

$$V_i = V_{out} y_i$$

y_i represents the volumetric fraction of CO and H_2 in the outlet gas, determined via gas chromatography; V_{out} denotes the flow rate of the outlet gas, measured using a soap film flowmeter.

The CO_2 utilization efficiency (UE) can be calculated using the following method:

$$UE = \frac{V_{CO_2\ to\ CO}}{V_{CO_2\ consumed}}$$

$V_{CO_2\ to\ CO}$ represents the consumption rate of CO_2 in the reaction for CO production;

According to the stoichiometric relationship of the reaction:

$$V_{CO_2\ to\ CO} = V_{CO}$$

$V_{CO_2\ consumed}$ represents the consumption rate of CO_2, which can be calculated using the following equation:

$$V_{CO_2\ consumed} = V_{in} - V_{CO_2}$$

V_{in} refers to the inlet gas flow rate; V_{CO_2} denotes the flow rate of residual CO_2 in the outlet gas, which can be calculated as follows:

$$V_{out} = V_{CO_2} + V_{CO} + V_{H_2}$$

The turnover frequency (TOF) value of the electrocatalyst was calculated as:

$$TOF = \frac{n_{CO}}{m\omega/M} \times 3600$$

M is the molar mass of Co, m represents the mass of the catalyst loaded on the electrode, ω is the mass fraction of the active sites.

Definition of $EDLC_{Co}$.

The effective electrochemical double-layer capacity ($EDLC_{Co}$) is defined as follows:

$$EDLC_{Co} = \frac{C_{dl}}{\omega}$$

C_{dl} refers to the double-layer capacitance of the catalyst, ω is the mass fraction of the active sites.

In-situ ATR-FTIR spectroscopy measurement

In this study, an in-situ attenuated total reflection Fourier transform infrared (ATR-FTIR) spectroscopy setup was employed, utilizing a modified electrochemical cell supplied by Shanghai Yuanfang Tech. The system incorporated a Thermo Nicolet IS50 spectrometer equipped with a mercury-cadmium-telluride (MCT) detector cooled with liquid nitrogen. A

thin gold film (~50 nm) plated on a silicon crystal served as the working electrode, onto which a catalyst-containing ink was deposited. The electrochemical cell operated in a three-electrode configuration, with a platinum mesh as the counter electrode and an Ag/AgCl electrode as the reference. The experiments were performed in a 0.25 M K_2SO_4 solution (pH = 1), with ATR-FTIR spectra recorded every 40 seconds. Prior to initiating the measurements, a baseline spectrum was obtained under open circuit conditions. All applied potentials were subsequently standardized to the reversible hydrogen electrode (RHE) scale to facilitate data consistency and comparison.

Supplementary Materials

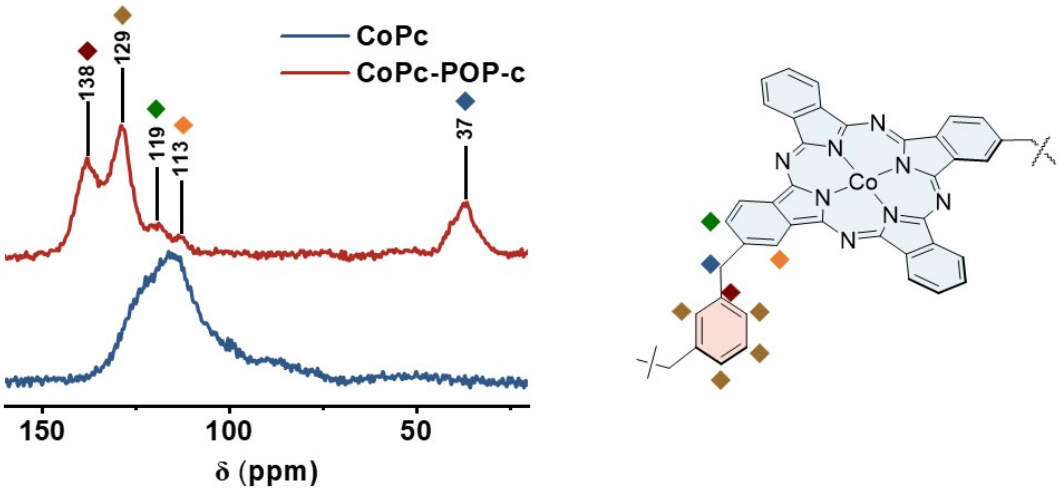

Figure S1. Solid-state ^{13}C NMR spectra of CoPc-POP-c and CoPc.

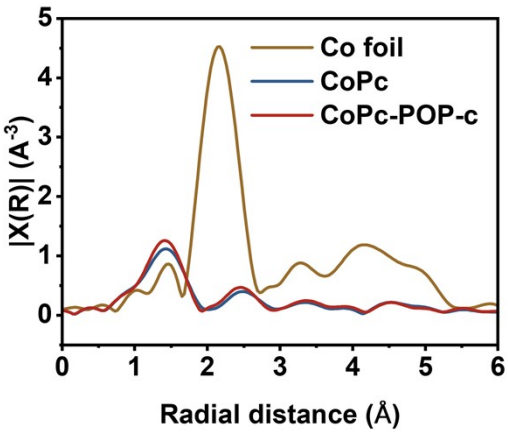

Figure S2. The EXAFS spectra of CoPc-POP-c and CoPc.

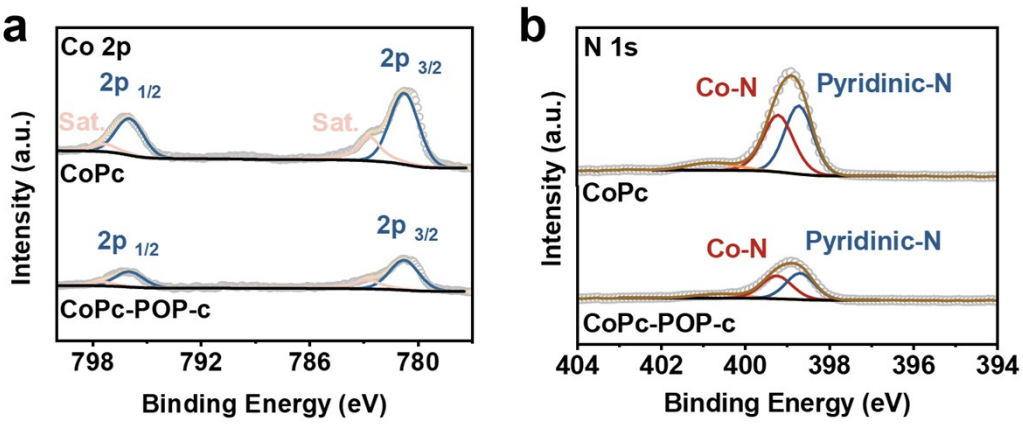

Figure S3. (a) The Co 2p and (b) N 1s XPS spectra of CoPc-POP-c and CoPc.

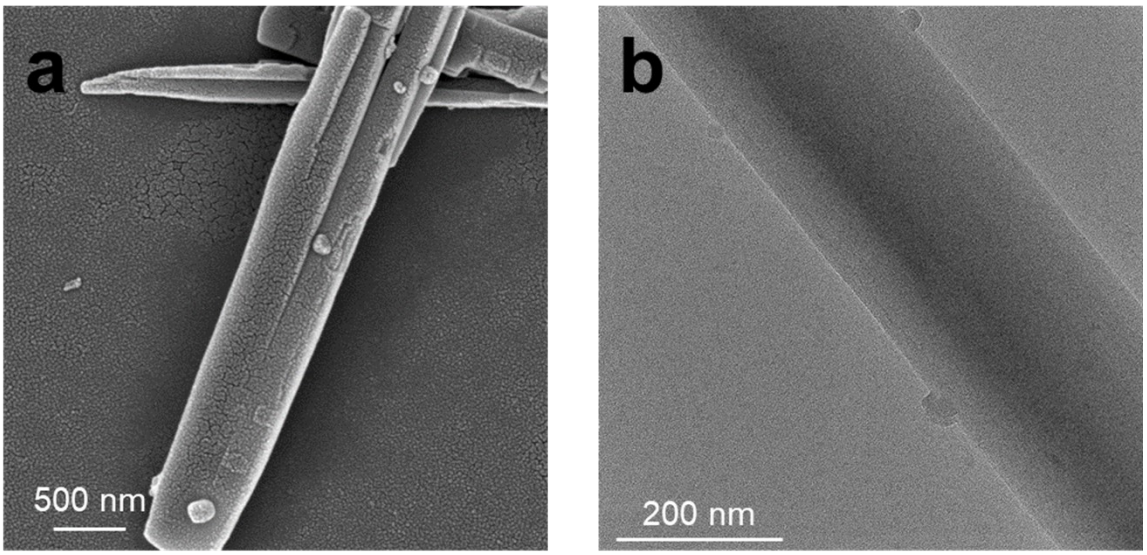

Figure S4. (a) SEM and (b) TEM images of the raw CoPc.

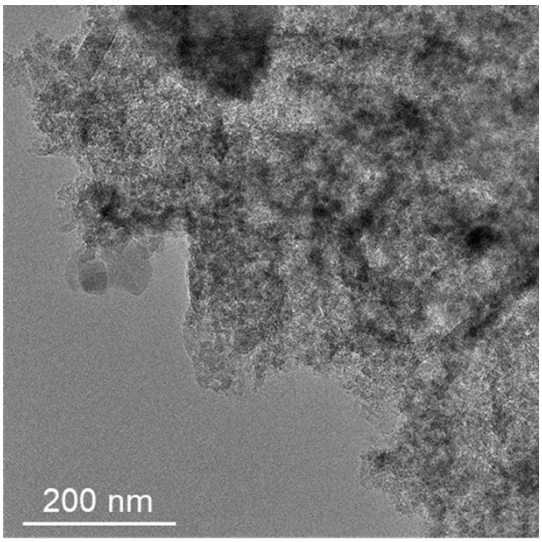

Figure S5. TEM image of the CoPc-POP-c

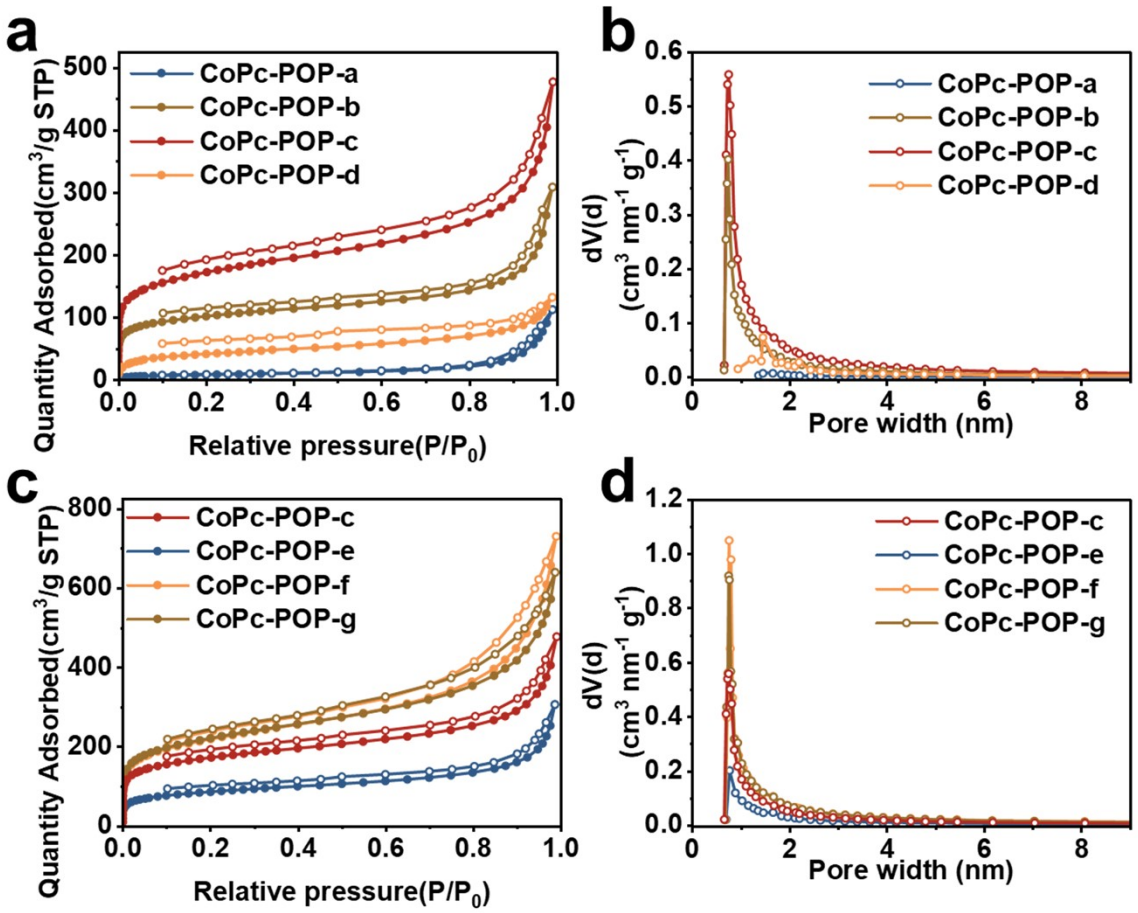

Figure S6. (a) Nitrogen adsorption and desorption isotherms and (b) pore width distribution of CoPc-POP-a-d. (c) Nitrogen adsorption and desorption isotherms and (d) pore width distribution of CoPc-POP-e-g and c.

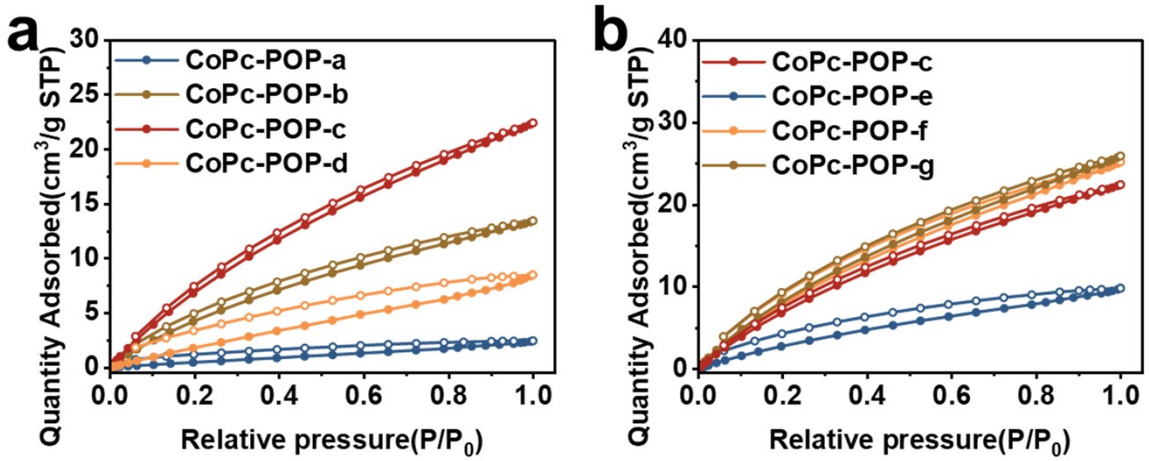

Figure S7. CO_2 adsorption and desorption isotherms of CoPc-POP (a) a-d, (b) e-g and c.

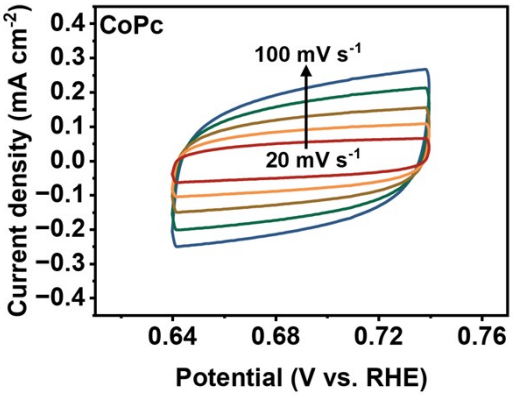

Figure S8. Cyclic voltammetry curves of CoPc.

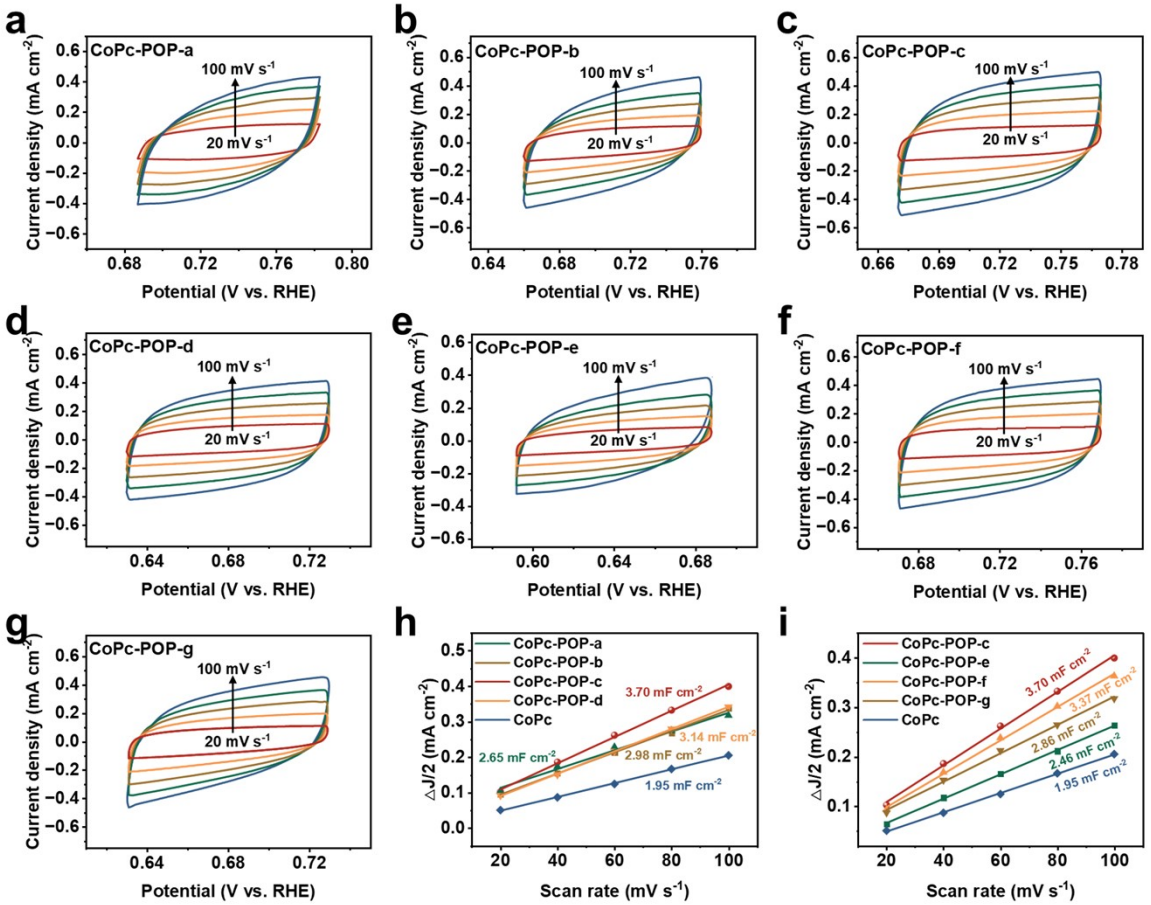

Figure S9. (a-g) Cyclic voltammetry curves of CoPc-POP-a-g at various scan rates. (h-i) Measured double-layer capacitance of the as-prepared catalysts.

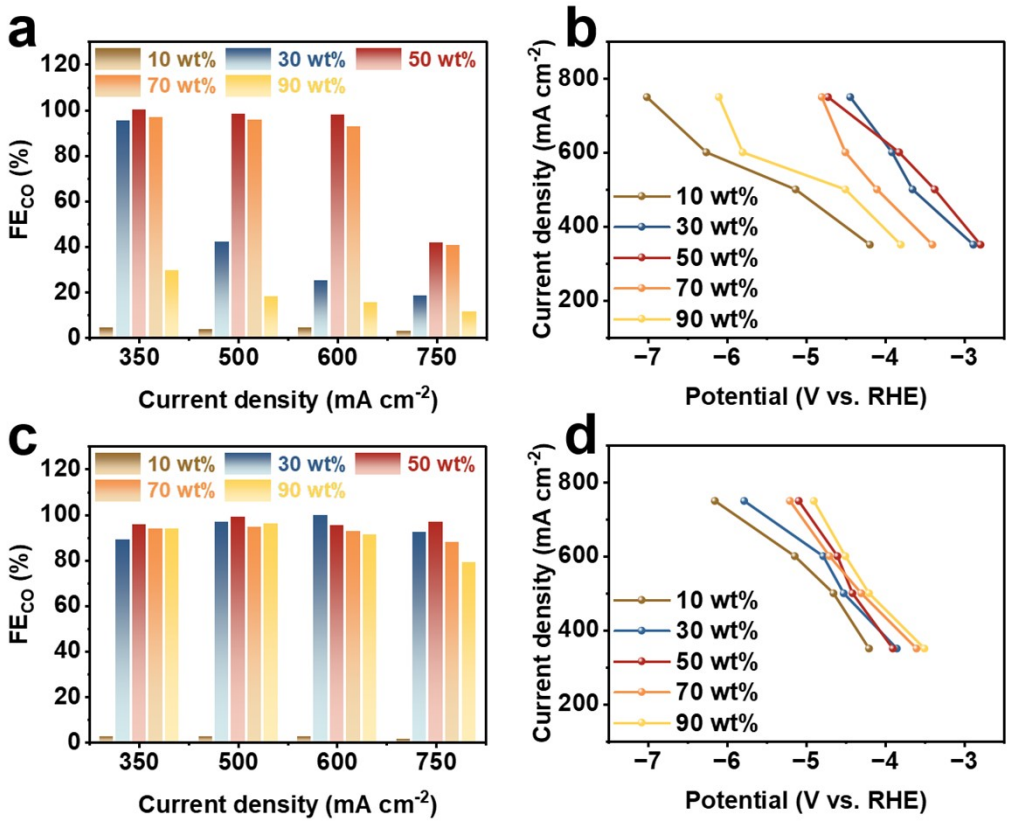

Figure S10. The variation in (a) FE_{CO} and (b) potential of CoPc with varying amounts of carbon black addition. The variation in (c) FE_{CO} and (d) potential of CoPc-POP-c with varying amounts of carbon black addition.

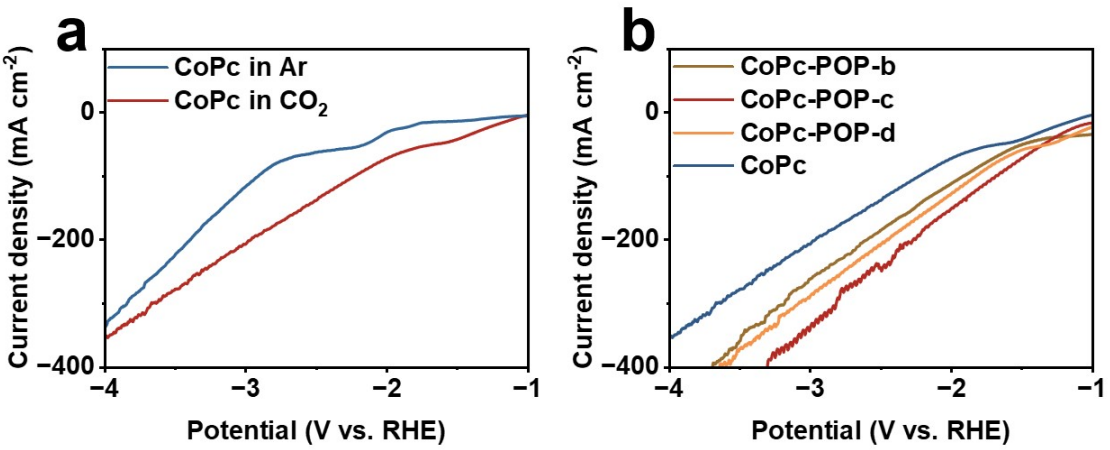

Figure S11. (a) LSV curves for CoPc in the Ar and CO_2 atmosphere. (b) LSV curves for CoPc-POP-b-d and CoPc in the CO_2 atmosphere.

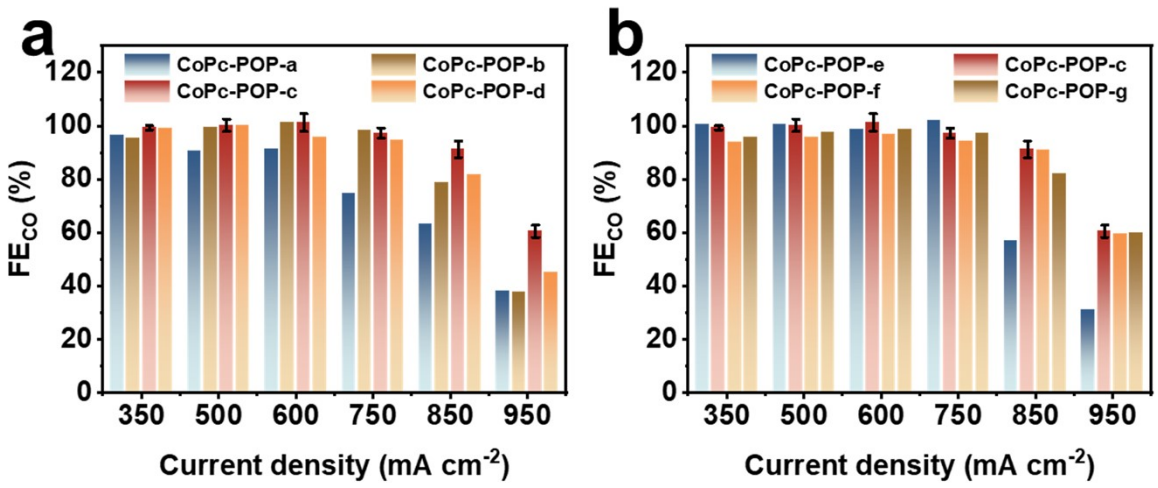

Figure S12. FE_{CO} of CoPc-POP (a) a-d, (b) e-g and c under various current densities.

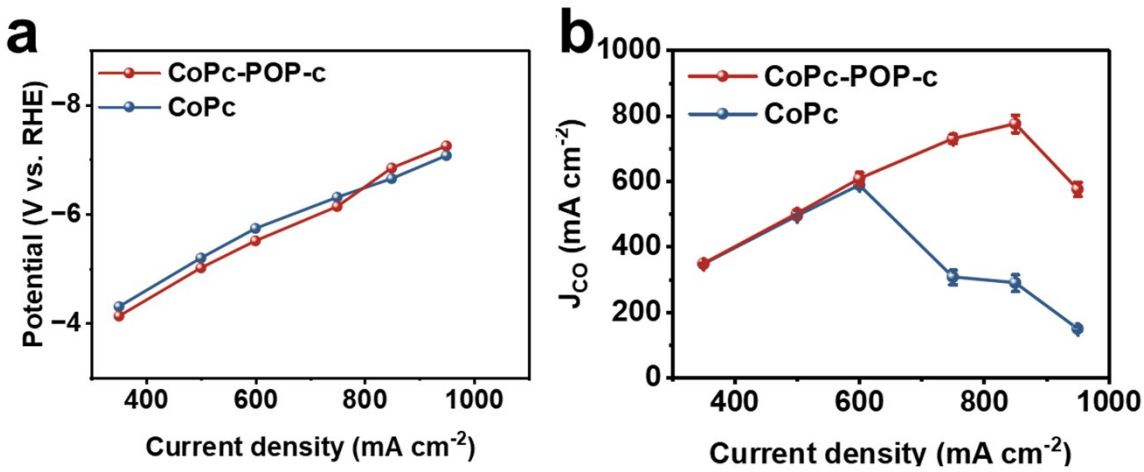

Figure S13. Comparison of (a) potential and (b) CO partial current density between CoPc-POP-c and CoPc at various current densities.

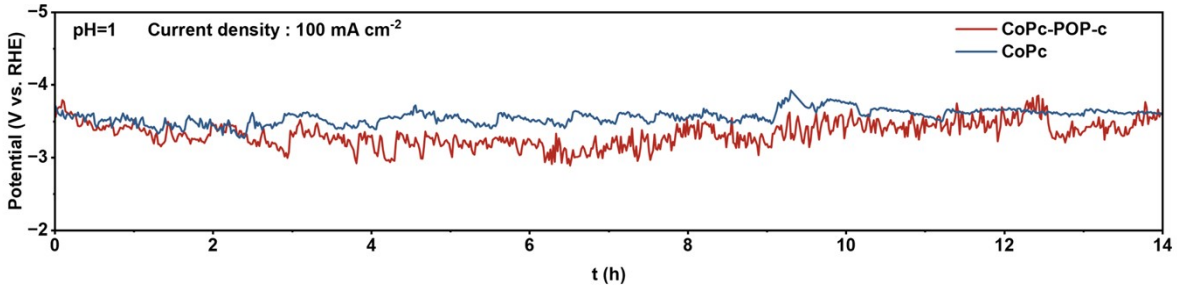

Figure S14. Potential variation of CoPc-POP-c and CoPc during long-term testing at 100 mA cm^{-2} in acidic media.

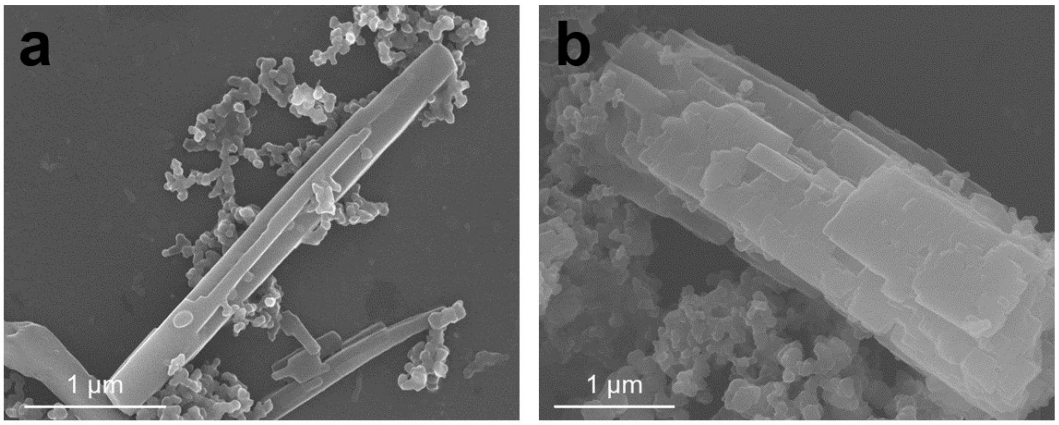

Figure S15. SEM images of CoPc (a) pre- and (b) post-electrolysis.

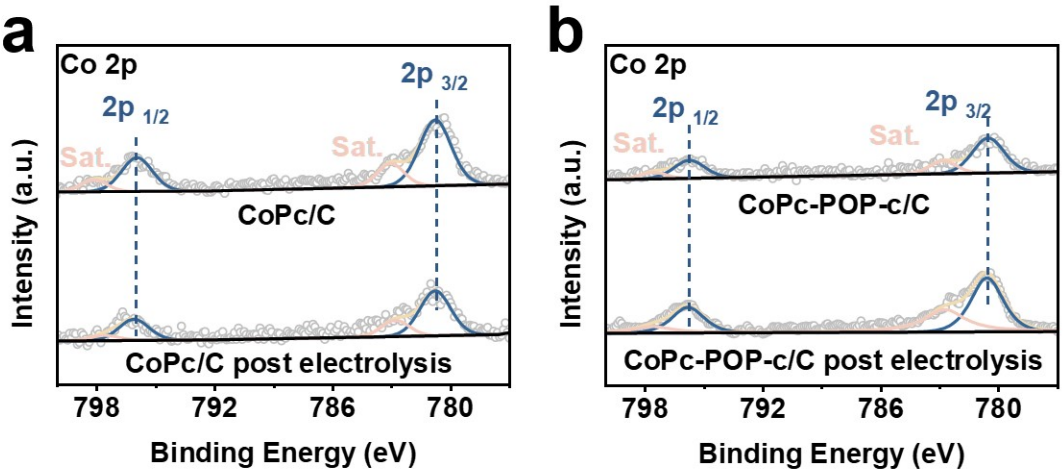

Figure S16. Co 2p XPS spectra of (a) CoPc/C electrode and (b) CoPc-POP-c/C electrode pre- and post-electrolysis.

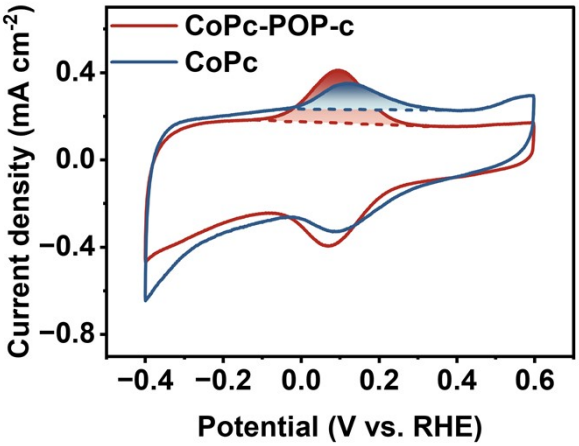

Figure S17. Cyclic voltammograms of the CoPc-POP-c and CoPc in a 0.5 M $KHCO_3$ electrolyte under N_2.

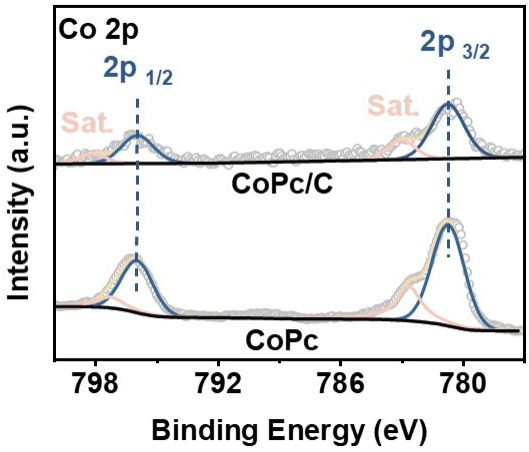

Figure S18. Co 2p XPS spectra of the CoPc electrode and the CoPc/C electrode.

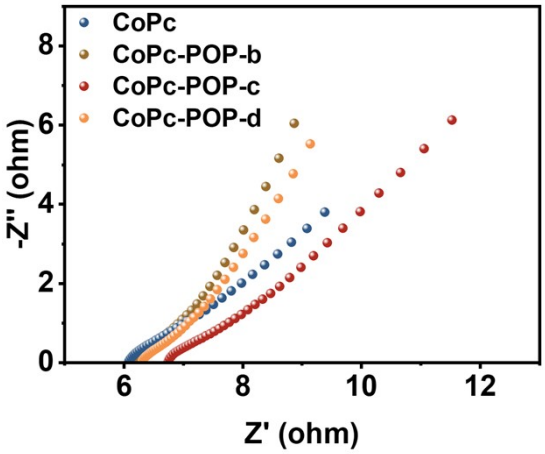

Figure S19. Electrochemical impedance spectroscopy fitting curve of CoPc-POP-b-d and CoPc.

Table S1. Fabrication of CoPc POPs through hyper-crosslinking using different ratios of benzene, FDA, and $FeCl_3$.

Sample	Benzene (equiv.)	$FeCl_3$ (equiv.)	FDA (equiv.)
CoPc-POP-a	0	20	20
CoPc-POP-b	3	20	20
CoPc-POP-c	10	20	20
CoPc-POP-d	30	20	20
CoPc-POP-e	10	9	9
CoPc-POP-f	10	40	40
CoPc-POP-g	10	60	60

Table S2. Metal content analysis and BET surface area of CoPc-POP-a-g.

Sample	Metal content (%)	S_{BET} (m^2 g^{-1})
CoPc-POP-a	4.35	30
CoPc-POP-b	4.98	375
CoPc-POP-c	2.75	628
CoPc-POP-d	2.69	153
CoPc-POP-e	5.49	311
CoPc-POP-f	2.70	793
CoPc-POP-g	2.38	803

Table S3. C_{dl} and the calculated $EDLC_{Co}$ of CoPc-POP-a-g and CoPc.

Sample	C_{dl} (mF cm^{-2})	$EDLC_{Co}$ (mF cm^{-2})
CoPc	1.95	20.1
CoPc-POP-a	2.65	60.9
CoPc-POP-b	2.98	59.8
CoPc-POP-c	3.7	134.5
CoPc-POP-d	3.14	116.7
CoPc-POP-e	2.46	44.8
CoPc-POP-f	3.37	124.8
CoPc-POP-g	2.86	120.2

Table S4. Comparison of CO_2RR performance between CoPc-POP-c catalyst and previously reported catalysts.

Catalyst	FE_{CO} (%)	j_{CO} (mA cm^{-2})	Electrolyte	Reference
CoPc-POP-c	91.2	775.5	0.25 M K_2SO_4 +H_2SO_4 (pH=1)	This work
CoPc-POP-c	97.3	729.8	0.25 M K_2SO_4 +H_2SO_4 (pH=1)	This work
$Ni_{NC\&SA}$/N-C	99.5	800	1.0 M KCl+H_2SO_4 (pH=2)	[1]
CoTAAPc@CNT-12	93.3	568.6	3.0 M KCl + 0.05 M H_2SO_4 (pH=1)	[2]
NiPc-OMe MDE	100	400	0.40 M K_2SO_4 + 0.10 M H_2SO_4 (pH=0.47)	[3]
Ni-SAC-800	98.8	296.4	1.5 M KCl (pH=2)	[4]
PcNi-im	~100	320	3 M KCl + 0.01 M H_2SO_4 (pH≈1)	[5]
c-Co SAC	91	273	1 M KCl + 0.05 M H_2SO_4 (pH=1)	[6]
Ni-N-C-10	100	250	1 M Cs_2SO_4 + H_2SO_4 (pH=2)	[7]
Cu/Ni-NC	99	190	Phosphate buffer (pH=3)	[8]

References

1. Y. Li, X. Cao, Q. Chen, R. Pan, J. Zhang, G. Meng, Y. Yang, Y. Li, J. Mao and W. Chen, *Small*, 2024, **20**, e2405367.
2. Q. Zhang, C. B. Musgrave, Y. Song, J. Su, L. Huang, L. Cheng, G. Li, Y. Liu, Y. Xin, Q. Hu, G. Ye, H. Shen, X. Wang, B. Z. Tang, W. A. Goddard and R. Ye, *Nature Synthesis*, 2024, **3**, 1231-1242.
3. Z. Jiang, Z. Zhang, H. Li, Y. Tang, Y. Yuan, J. Zao, H. Zheng and Y. Liang, *Advanced Energy Materials*, 2022, **13**, 2203603.
4. Q. Wu, J. Liang, L. L. Han, Y. B. Huang and R. Cao, *Chem Commun (Camb)*, 2023, **59**, 5102-5105.
5. M. D. Zhang, J. R. Huang, W. Shi, P. Q. Liao and X. M. Chen, *Angew Chem Int Ed Engl*, 2023, **62**, e202308195.
6. J. Wang, X. Chen, Z. Yang, J.-D. Xiao, C. Qin, Z. Yan, Z. Wang, J. Yang and J. Wang, *Journal of Materials Chemistry A*, 2024, **12**, 9147-9154.
7. X. Sheng, W. Ge, H. Jiang and C. Li, *Adv Mater*, 2022, **34**, e2201295.
8. L. Zhang, J. Feng, S. Liu, X. Tan, L. Wu, S. Jia, L. Xu, X. Ma, X. Song, J. Ma, X. Sun and B. Han, *Adv Mater*, 2023, **35**, e2209590.